# Effect of initial pressure on laminar combustion characteristics of hydrogen enriched natural gas

Haiyan Miao*, Qi Jiao, Zuohua Huang, Deming Jiang

*State Key Laboratory of Multiphase Flow in Power Engineering, School of Energy and Power Engineering, Xi'an Jiaotong University, China Xi'an 710049*

## ARTICLE INFO

## ABSTRACT

Flame propagation of premixed natural gas–hydrogen–air mixtures was studied in a constant volume combustion bomb. Laminar burning velocities and mass burning fluxes were obtained under various hydrogen fractions and equivalence ratios with various initial pressures, while flame stability and their influencing factors (Markstein length, density ratio and flame thickness) were obtained by analyzing the flame images at various hydrogen fractions, initial pressures and equivalence ratios. The results show that hydrogen fraction, initial pressure as well as equivalence ratio have combined influence on both unstretched laminar burning velocity and flame instability. Meanwhile, according to flame propagation pictures taken by the high speed camera, flame stability decreases with the increase of initial pressures; for given equivalence ratio and hydrogen fraction, flame thickness is more sensitive to the variation of the initial pressure than to that of the density ratio.

## 1. Introduction

Investigation on alternative fuels such as natural gas (NG), hydrogen, methanol and ethanol is important both from an environmental and resource perspective, much of the activity now being centered on applications to transport engines. One of the most plentiful alternative fuels is NG [1], in contrast to the inevitable decline in petrol resources. Legislation in the USA and Europe has tightened 'local' emissions standards and, while the Kyoto protocol has emphasized the need to limit the 'global' problem of high carbon dioxide products. Gas fuels are beneficial in both these aspects.

NG, which is predominantly methane, has already been used in passenger cars. However, due to its long ignition delay period and rather slow flame propagation speed at lean conditions, NG fueled internal combustion engines suffer from low thermal efficiency, high cycle-to-cycle variation and increased unburned hydrocarbon emissions when operating at low engine load. One of the effective methods to solve the problem is to add fuel with faster burning velocity. As a renewable gaseous fuel, hydrogen seems to be the best candidate, which is difficult to apply directly into transport engines due to safety and economic reasons. Engine testing showed that using hydrogen enriched NG leaner combustion can be achieved with improved engine performance and reduced emissions [2]. To achieve better usage of this blended fuel, a better fundamental understanding of its combustion processes is required.

Fundamental study on laminar burning characteristics of a fuel provides basic information for engine design and the development of reliable incylinder process models. The laminar burning velocity and Markstein length are important

---

*Corresponding author. Tel.: +86 29 82665075; fax: +86 29 82668789.
E-mail addresses: hymiao@mail.xjtu.edu.cn (H. Miao), flowers@stu.xjtu.edu.cn (Q. Jiao), zhhuang@mail.xjtu.edu.cn (Z. Huang), dmjiang@mail.xjtu.edu.cn (D. Jiang).

**Nomenclature**

| | |
|---|---|
| $A$ | flame area, m$^2$ |
| $f$ | mass burning flux, g cm$^{-1}$ s$^{-1}$ |
| $L$ | molar number of air |
| $L_b$ | markstein length of burned gases |
| $p_o$ | initial mixture pressure, MPa |
| $r_u$ | flame radius, mm |
| $R_{H_2} = \frac{H_2(vol\%)}{NG(vol\%)+H_2(vol\%)}$ | hydrogen volumetric fraction in blended fuel |
| $S_l$ | unstretched flame speed, m/s |

| | |
|---|---|
| $S_n$ | stretched flame speed, m/s |
| $t$ | time, s |
| $T_o$ | initial temperature, K |
| $u_l$ | unstretched laminar burning velocity, m/s |
| $u_n$ | stretched laminar burning velocity, m/s |
| $u_{nr}$ | stretched mass burning velocity, m/s |
| $\rho_b$ | density of burned gases, kg/m$^3$ |
| $\rho_u$ | density of unburned gases, kg/m$^3$ |
| $\alpha$ | flame stretch rate, s$^{-1}$ |
| $\phi$ | equivalence ratio |
| $\delta_l$ | flame thickness, mm |
| $v$ | kinematic viscosity of unburned gas, m$^2$/s |

parameters representing laminar burning characteristics, in which the Markstein length reflects the stability of small radius flame. Regarding about gaseous fuels, combustion of methane and hydrogen has been studied intensively [e.g., 3,4]. Using spherical flame gas measurement, [5] studied laminar burning velocity of NG. Yu et al. [6] and Halter et al. [7] investigated the combustion of hydrogen–methane mixtures and found that adding hydrogen can effectively increase burning velocities of the mixtures. Law et al. [8] gave the flame propagation photos of a small amount of hydrogen into methane (methane content in the volume is less than 15%) and concluded that a high addition rate of hydrogen increases the instability of the flame. Huang et al. [9] studied the impact of hydrogen fraction on laminar burning velocities of NG–hydrogen–air mixtures at ambient pressure and room temperature. Kwon et al. [10] studied the effect of pressure on the combustion characteristics of propane–air and hydrogen–oxygen–nitrogen in a high pressure constant volume combustion chamber. It was found that with the increase of initial pressure, the flame thickness is reduced, encouraging flame instability. There is little reported work about the effect of initial pressure on the combustion of NG–hydrogen–air mixtures so far.

This paper intended to provide fundamental combustion information which can be used directly in designing combustion systems such as turbine engines and internal combustion engines fuelled with hydrogen enriched NG with improved lean burn operation. NG is employed rather than methane as pure methane seldom exists in nature resources. By employing a constant volume combustion bomb and high speed Schlieren photography, laminar burning characteristics of NG–hydrogen–air mixtures with hydrogen fraction of 20%, 40%, 60%, 80% and 100% (in volume) were studied at various equivalence ratios under different initial pressures of 0.08, 0.1, 0.15 and 0.2 MPa, respectively. Flame stability as well as its influencing factors was obtained by the combination of flame propagation photos, laminar burning velocity and Markstein length.

## 2. Experimental setup

The experiment was conducted in a constant volume combustion bomb with schlieren photography. The combustion bomb used is a cylindrical type with the diameter of 130 mm and the length of 130 mm, as shown in Fig. 1. Two sides of the bomb are transparent to provide optical access, allowing observation of the combustion inside. The flame propagation photos are recorded by a Redlake HG-100 K high speed CCD camera, operating at 10 000 pictures per second with a schlieren optical system, and the detailed experimental setup about the schlieren system is given in Fig. 2.

As shown in Fig. 2, the inlet/outlet valve is used to let fresh air or combustion product in or out. In the experiments, the initial pressure is set at 0.08, 0.1, 0.15 and 0.2 MPa, respectively, with constant initial temperature at 300 K. The combustible mixture is prepared by adding NG, hydrogen and air at the calculated partial pressures according to its corresponding hydrogen fraction and equivalence ratio. Enough time (5 min) is required to obtain the quiescent mixture. The fuel–air mixture is then ignited by a couple of centrally located electrodes and a standard capacitive discharge ignition system is used to produce the spark. In this study, the ignition energy is 45 mJ. The pressure inside the bomb is recorded by a piezoelectric Kistler pressure transducer with a resolution of 0.01 kPa.

In this work, hydrogen with purity of 99.995% was used and the hydrogen fraction is defined as the volume fraction of the hydrogen in the hydrogen enriched NG mixture. The NG constitution is listed in Table 1. Considering the formula of NG as $C_\alpha H_\beta O_\gamma$, it can be calculated that $\alpha$ is 1.01523, $\beta$ is 3.928084 and $\gamma$ is 0.05086. The combustible mixture in bomb can be expressed as $xC_\alpha H_\beta O_\gamma + (1-x)H_2 + L(O_2 + 3.762N_2)$, and the equivalence ratio of NG–hydrogen–air mixture is defined as

$$\phi = \left(\left(\alpha + \frac{\beta}{4} - \frac{\gamma+1}{2}\right)x + \frac{1}{2}\right)/L.$$

## 3. Combustion analyses theory

The laminar burning velocity and Markstein length can be deduced from schlieren photographs as described by Bradley et al. [11]. For a spherically expanding flame, the stretched flame velocity ($S_n$) is derived from the flame radius versus time data as
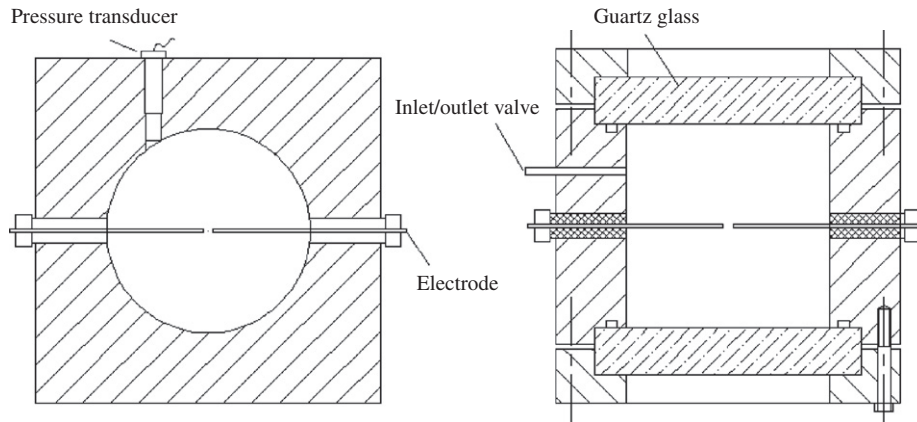
$$S_n = \frac{dr_u}{dt} \tag{1}$$

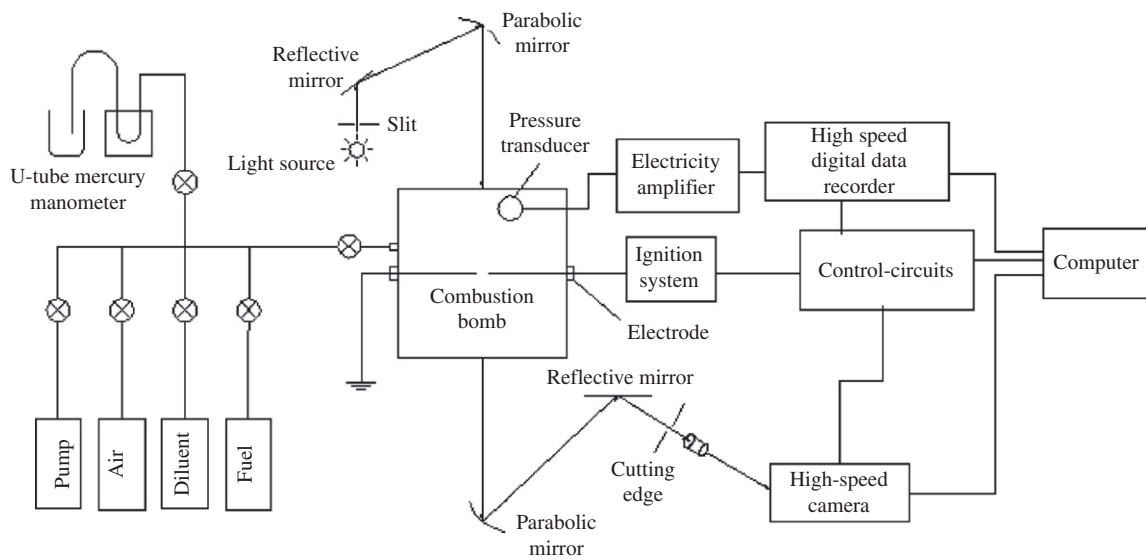**Fig. 1 – Structure of the constant volume combustion bomb.**



**Fig. 2 – Experimental system arrangement.**

**Table 1 – Constitution of natural gas**

| Items | CH$_4$ | C$_2$H$_6$ | C$_3$H$_8$ | N$_2$ | CO$_2$ | Others |
|---|---|---|---|---|---|---|
| Volumetric fraction (%) | 96.160 | 1.096 | 0.136 | 0.001 | 2.540 | 0.067 |

where $r_u$ is the radius of flame in schlieren photographs and $t$ is the time. Note that the flame radius is analyzed beyond 6 mm at which the spark effects could be discounted.

Flame stretch rate $\alpha$ in a quiescent mixture is defined as

$$\alpha = \frac{d(\ln A)}{dt} = \frac{1}{A}\frac{dA}{dt} \qquad (2)$$

where $A$ is the area of flame. For a spherically outwardly expanding flame front, the flame stretch rate can be simplified as

$$\alpha = \frac{1}{A}\frac{dA}{dt} = \frac{2}{r_u}\frac{dr_u}{dt} = \frac{2}{r_u}S_n \qquad (3)$$

In respect to the early stage of flame expansion, there exists a linear relationship between the flame speeds and the flame stretch rates [11], that is,

$$S_l - S_n = L_b\alpha \qquad (4)$$

where $L_b$ is the Markstein length of burned gases. From Eqs. (1) and (3), the stretched flame speed ($S_n$) and flame stretch rate ($\alpha$) can be calculated.

The unstretched flame speed, $S_l$, can be obtained as the intercept value at $\alpha = 0$, in the plot of $S_n$ against $\alpha$, and the burned gas Markstein length $L_b$ is the slope of $S_n$–$\alpha$ curve. Markstein length can reflect the stability of flame.

Positive value of $L_b$ indicates that the flame speed decreases with the increase of flame stretch rate, in the case, if any kinds of protuberances appear at flame front (stretch increasing), the flame speed at flame protruding position will be suppressed, and this makes the flame stable. In contrast to this, negative value of $L_b$ means that the flame speed increases with the increase of flame stretch rate, in the case, if any kinds of protuberances appear at flame front, the flame speed at flame protruding position will be increased, and this increases the instability of flame [11]. When the observation is limited to the initial part of the flame expansion, where the pressure does not vary significantly yet, then a simple relationship links the spatial flame velocity ($S_l$) to unstretched laminar burning velocity ($u_l$) given as follows,

$$u_l = \rho_b S_l / \rho_u \tag{5}$$

where $\rho_b$ and $\rho_u$ are the densities for burned gases and unburned gases. The value of $\rho_u$ is determined directly by ideal-gas equation of state while that of $\rho_b$ was found from the calculated properties of the equilibrated adiabatic products [12].

Eq. (6) is used to determine the stretched laminar burning velocity $u_n$ and the stretched mass burning velocity $u_{nr}$ is given in Eq. (7),

$$u_n = S\left[S_n \frac{\rho_b}{\rho_u}\right] \tag{6}$$

$$u_{nr} = \frac{\rho_b}{\rho_b - \rho_u}(u_n - S_n) \tag{7}$$

In Eq. (6) $S$ is a rectified function and it depends upon the flame radius and the density ratio, and accounts for the effect of the flame thickness on the mean density of the burned gases. The expression of $S$ in the present study used the formula given by Bradley et al. [11]:

$$S = 1 + 1.2\left[\frac{\delta_l}{r_u}\left(\frac{\rho_u}{\rho_b}\right)^{2.2}\right] - 0.15\left[\frac{\delta_l}{r_u}\left(\frac{\rho_u}{\rho_b}\right)^{2.2}\right]^2 \tag{8}$$

## 4. Results and discussions

### 4.1. Laminar burning velocity

Fig. 3 gives the unstretched laminar burning velocity and the mass burning flux versus hydrogen fraction under various initial pressures at three equivalence ratios representing lean,
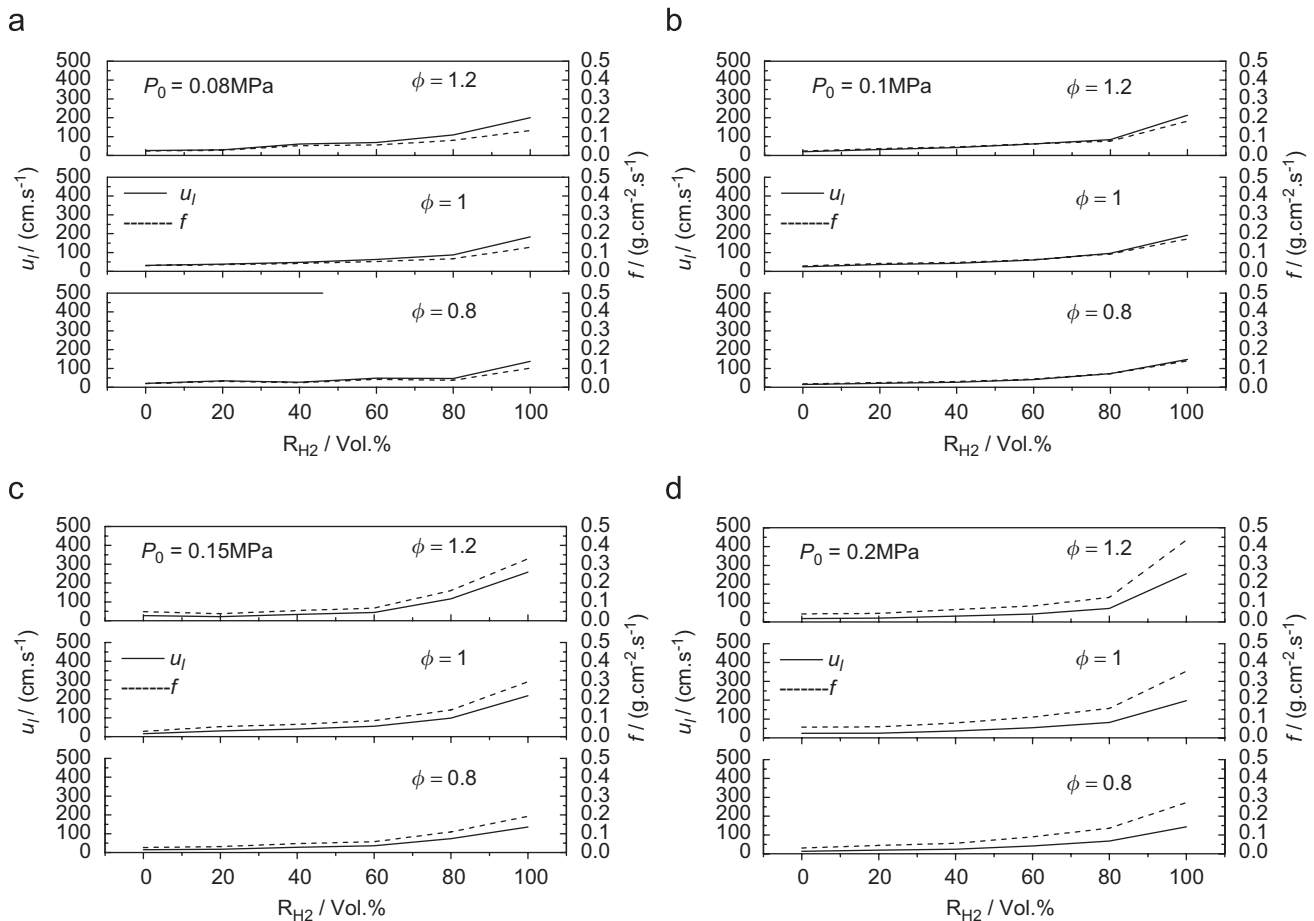


Fig. 3 – Effects of initial pressure, hydrogen fraction and equivalence ratio on unstretched laminar burning velocities and mass burning fluxes.

stoichiometric and rich mixtures, respectively. The results show that both unstretched laminar burning velocity and the mass burning flux increase with the increase of hydrogen fraction. Within the range of the experiments, the higher the hydrogen fraction is, the larger they increase. For rich mixture combustion, the increase rate of mass burning flux is higher than that of lean and stoichiometric mixture combustion. This shows that hydrogen addition is especially effective in increasing the burning velocity at rich conditions.

Experimental results prove that hydrogen fraction, equivalence ratio and initial pressure have integrated effects on laminar burning velocity of hydrogen enriched NG. As shown in Fig. 3, with high hydrogen fraction (80% in volume and above), initial pressure has extinguish effects on burning velocity. However, with the hydrogen fraction less than 80%, this effect is rather small, especially at low hydrogen fraction ($R_{H_2} = 20$ vol%). The effect of initial pressure at various equivalence ratios is rather complicated. Using the case of 80% fraction of hydrogen as an example. At stoichiometric condition the laminar burning velocity of the mixture is 2.2, 3.16, 5.04 and 2.72 times as large as that of NG with initial pressure of 0.08, 0.1, 0.15 and 0.2 Mpa, respectively. When $\phi = 0.8$, it is 1.9, 4.33, 3.93 and 4.35 times as large as that of NG with initial pressure of 0.08, 0.1, 0.15 and 0.2 MPa, respectively, and when $\phi = 1.2$, it is 3.27, 3.12, 3.26 and 3.0, respectively. As a summary, at rich conditions the laminar burning velocity declines with the increase of initial pressure, while at lean and stoichiometric conditions it tends to increase and then decrease with the increase of initial pressure within the range of the experiments.

Our experimental results indicated that increment of initial pressure can be either favorable or unfavorable to the flame propagation. Pressure has two effects on the flame: chemical (radical concentration) and thermal (flame temperature) [13]. On the one hand, it was reported that concentrations of the radicals such as H and OH are decreased with elevated pressure (e.g., [14]) and this causes that the flame speed tends to decline with the increase of initial pressure. On the other hand, increment of pressure will increase the temperature of the reaction zone, as a result increasing the flame speed. It will depend on the dominant factor to decide whether the increment of initial pressure is favorable or unfavorable to the flame speed.

### 4.2. Flame stability

The stability of premixed flame is influenced by both thermo-diffusive factor and hydrodynamic factor [3,7]. At the initial stage of flame propagation, the thermo-diffusive factor plays a crucial role and with the further development of the flame, the hydrodynamic influence becomes stronger. Markstein length can be used to quantify the sensitivity of a flame on stretch [11]. As discussed before, positive Markstein length indicates that stretched flame propagation speed decreases with the increase of stretch rate, that is, the flame tends to restrain protuberances in the flame front and this tendency leads to a stable flame and vice versa. Based on analyzing schlieren photos obtained from the experiments, Markstein lengths were obtained. In this section, the effects of initial pressure on the flame stability will be discussed combining
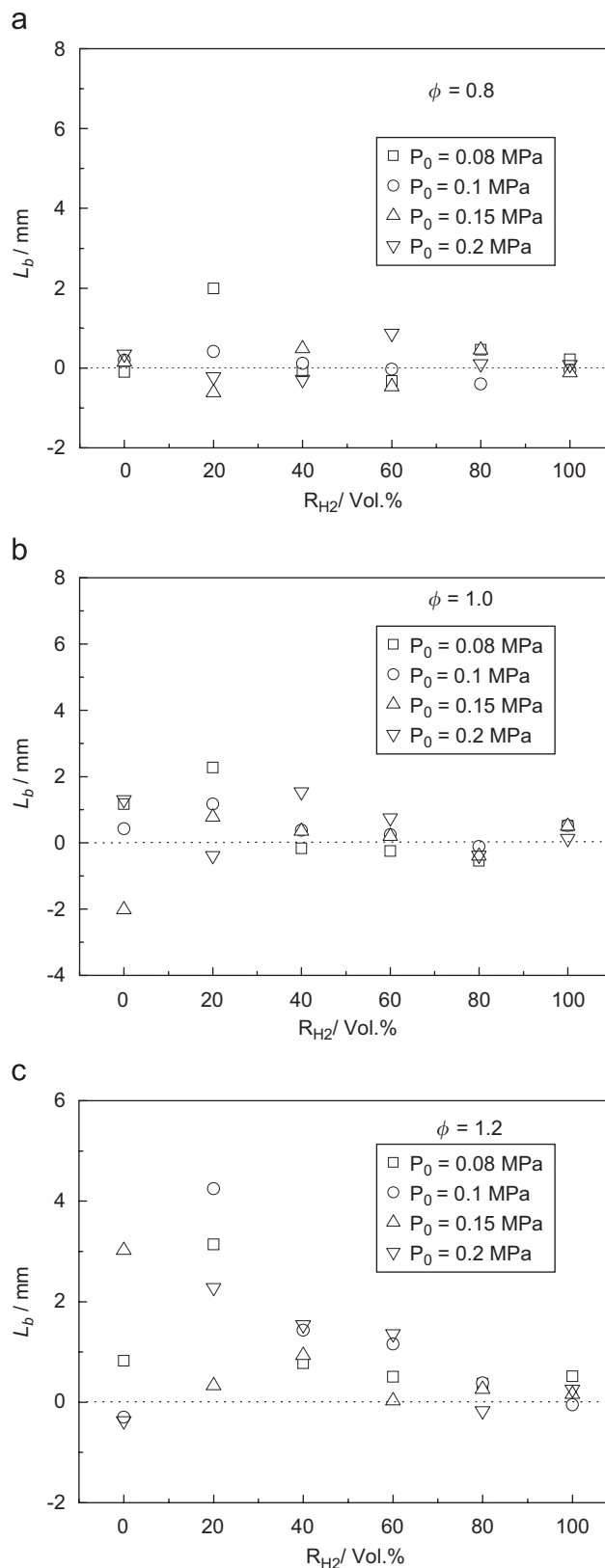


Fig. 4 – Effects of initial pressure, hydrogen fraction and equivalence ratio on Markstein length.

Markstein length and schlieren photos that provide evidence of the extent of flame instability.

Fig. 4 illustrates the relationship between Markstein length and hydrogen fraction at different equivalence ratios under various initial pressures. The Markstein length tends to decline with the increase of hydrogen fractions, which reveals that the flame stability decreases with the increase of hydrogen fractions. To the mixture with 20% fraction of hydrogen in NG, the Markstein length decreases with the increase of initial pressures, while for the mixtures with higher hydrogen fraction (that is 40%, 60%, 80% in volume), the Markstein number values near the boundary between flame stability and flame instability, which indicates that the flame tends to be instable with high hydrogen enrichment.

By analyzing the flame propagation schlieren photos of fuel mixtures with various hydrogen fractions under stoichiometric condition with initial pressures of 0.1 and 0.2 Mpa, respectively (as shown in Figs. 5 and 6), it was observed that flame propagates faster with higher hydrogen fraction. In the case of 20% hydrogen fraction, slight flaw and protrudence occur at the early stage and more flaw and protrudence are developed with the initial pressure of 0.2 MPa than that of 0.1 MPa. In the cases with higher hydrogen fraction, larger flaw and protrudence are observed at the early stage of flame propagation with higher initial pressure, resulting in cellular surface structure at the late stage of flame development. This reveals that flame stability decreases with the increase of the initial pressure. As well-developed flaws appear at the early

stage of the flame propagation for the mixtures with high hydrogen fractions, this indicates that the flame tends to be instable for the mixtures with high hydrogen fractions.

Fig. 7 compares the flame propagation schlieren photos of the fuel mixture with 20% hydrogen addition at different initial pressures and various equivalence ratios from lean to rich. With the initial pressure increases from 0.1 to 0.2 MPa, different phenomena were observed for the mixtures with different equivalence ratios: at lean condition, larger flaw and honeycomb-like surface are developed with higher initial pressure, while smooth surface is remained at both rich and stoichiometric conditions. It shows that at relatively lean conditions, flame stability is quite sensitive to the initial pressure for the mixture with low hydrogen enrichment; the higher the initial pressure is, the less stable the flame becomes. We also studied flame sensitivity of the mixtures with high hydrogen additions to the change of the initial pressure. As shown in Fig. 8, when the initial pressure increases from 0.1 to 0.2 MPa, the flames from lean to rich all have large flaw and honeycomb-like surface, especially in lean and stoichiometric conditions in which cases flame stability obviously decreases with the increase of the initial pressure.

By comparing Figs. 7 and 8, it was observed that with same initial pressure and equivalence ratio increase of hydrogen fraction of a fuel mixture decreases its flame stability; at rich conditions the increase of hydrogen fraction exerts less influence on flame stability comparing with that at lean and
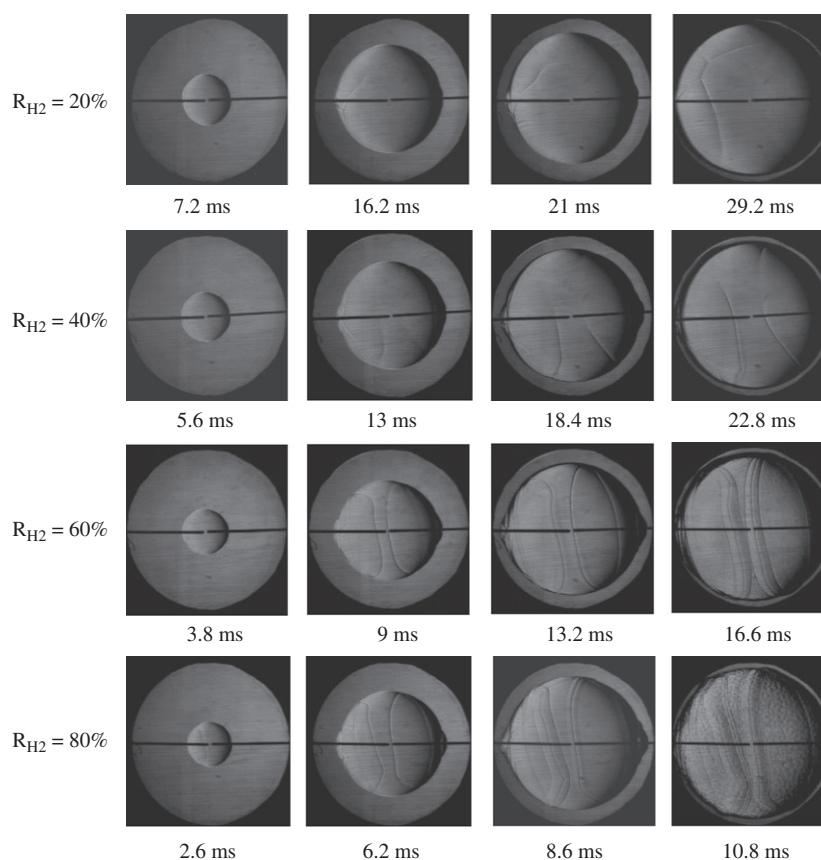


$R_{H2} = 20\%$    7.2 ms    16.2 ms    21 ms    29.2 ms

$R_{H2} = 40\%$    5.6 ms    13 ms    18.4 ms    22.8 ms

$R_{H2} = 60\%$    3.8 ms    9 ms    13.2 ms    16.6 ms

$R_{H2} = 80\%$    2.6 ms    6.2 ms    8.6 ms    10.8 ms

Fig. 5 – Schlieren photos of flame propagation at various hydrogen fractions ($\phi = 1.0$, $P_0 = 0.1$ MPa).
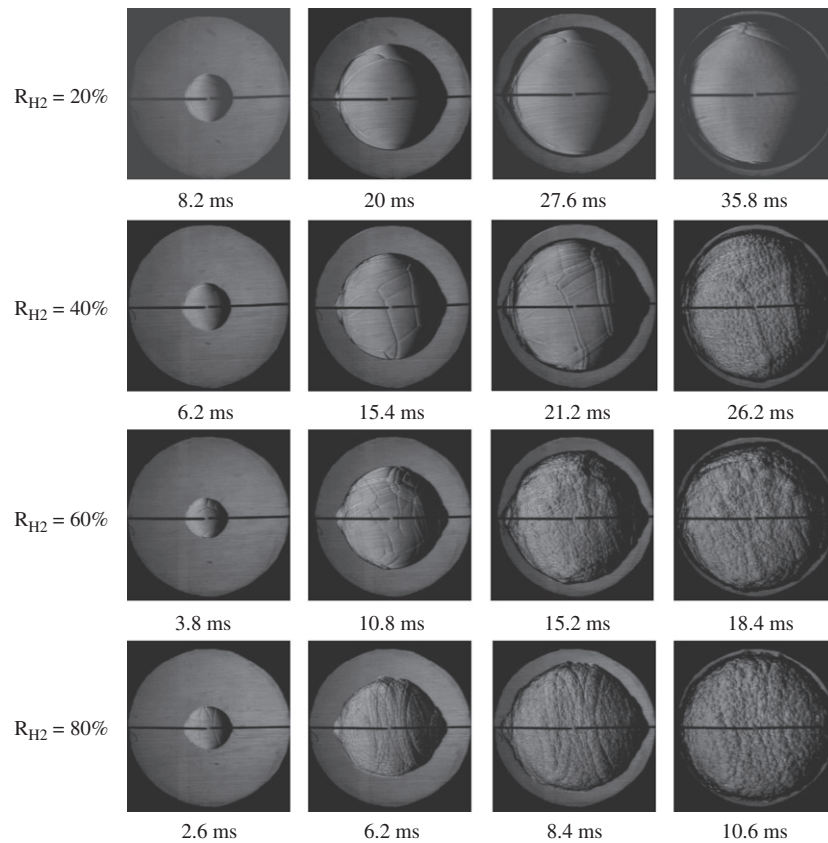
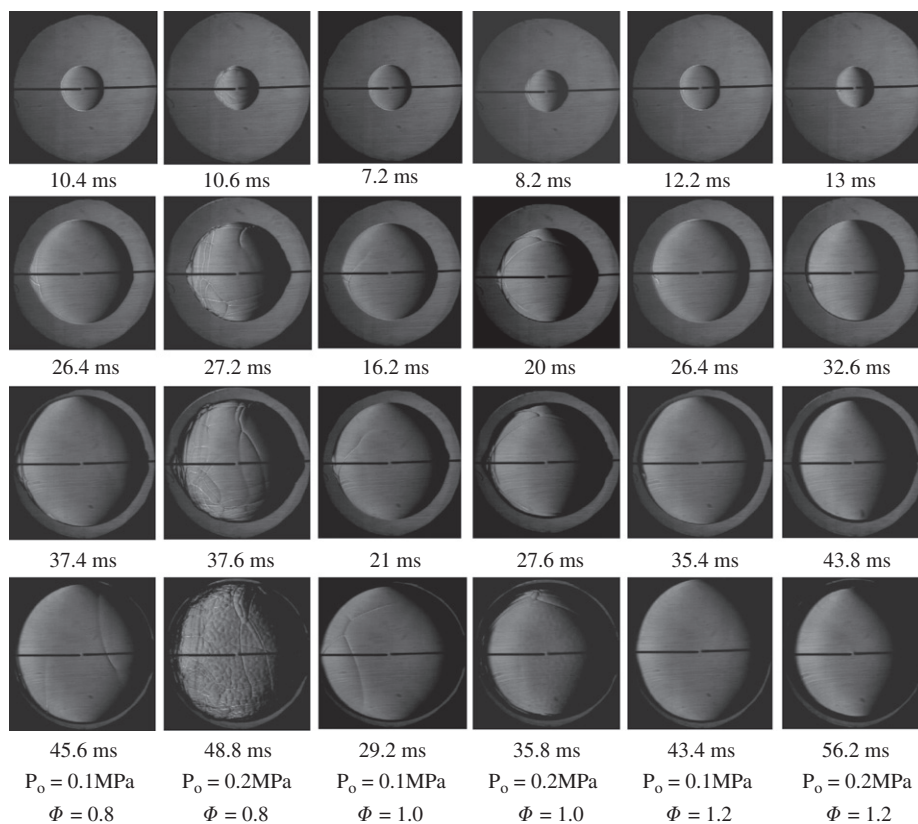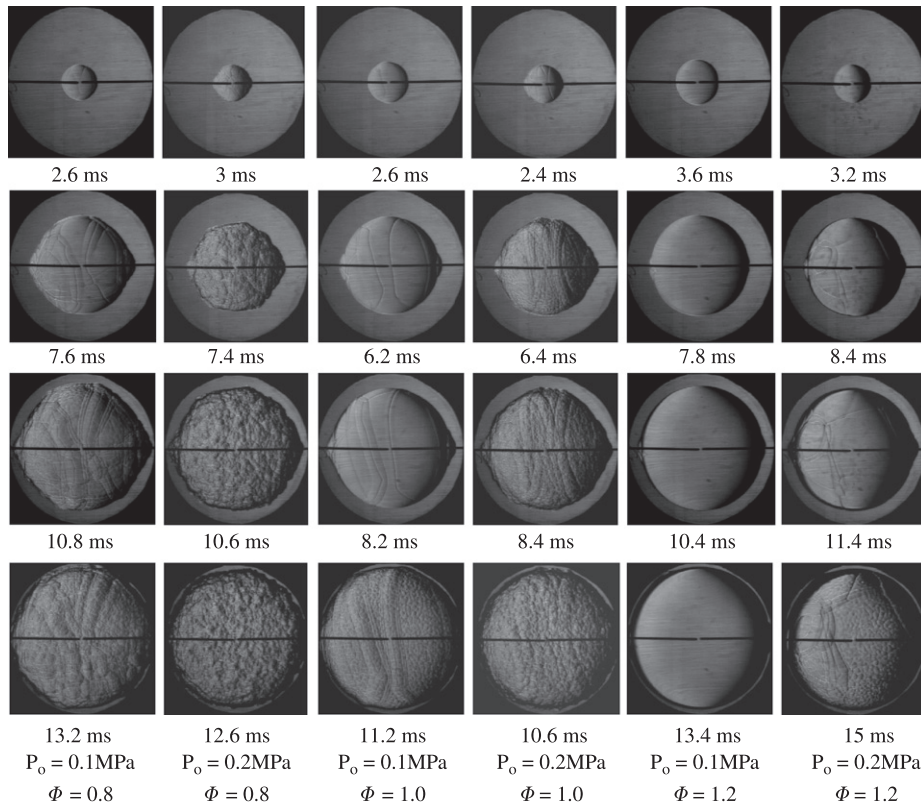**Fig. 6 – Schlieren photos of flame propagation at various hydrogen fractions ($\phi = 1.0$, $P_0 = 0.2$ MPa).**



**Fig. 7 – Schlieren photos of flame propagation at various initial pressures and equivalence ratios with 20 vol% hydrogen addition.**

| 2.6 ms | 3 ms | 2.6 ms | 2.4 ms | 3.6 ms | 3.2 ms |
| 7.6 ms | 7.4 ms | 6.2 ms | 6.4 ms | 7.8 ms | 8.4 ms |
| 10.8 ms | 10.6 ms | 8.2 ms | 8.4 ms | 10.4 ms | 11.4 ms |
| 13.2 ms | 12.6 ms | 11.2 ms | 10.6 ms | 13.4 ms | 15 ms |
| $P_o$ = 0.1MPa | $P_o$ = 0.2MPa | $P_o$ = 0.1MPa | $P_o$ = 0.2MPa | $P_o$ = 0.1MPa | $P_o$ = 0.2MPa |
| $\Phi$ = 0.8 | $\Phi$ = 0.8 | $\Phi$ = 1.0 | $\Phi$ = 1.0 | $\Phi$ = 1.2 | $\Phi$ = 1.2 |

**Fig. 8 – Schlieren photos of flame propagation at various initial pressures and equivalence ratios with 80 vol% hydrogen addition.**

stoichiometric conditions. Flame of rich mixtures has smooth surface with the increase of hydrogen fraction (from 20% to 80%) in both cases, revealing that increase of hydrogen fraction has slight effect on flame stability at rich conditions. But flame stability is visibly decreased for lean and stoichiometric mixtures. Moreover, with elevated initial pressure, increase of hydrogen fraction slightly changes flame stability of rich mixtures and visibly decreases flame stability of lean and stoichiometric mixtures. It is noted that elevated initial pressure advances the occurrence of flame instability featured with flaw and honeycomb-like surface (same hydrogen fraction and equivalence ratio).

According to [7], flame instability at early stage of flame propagation is mainly influenced by thermo-diffusive factor for constant volume combustion. With further expansion, hydrodynamic factor becomes dominant at large flame radius. For free diffusive flame, hydrodynamic instability is due to thermal expansion of the gas [3], which can be reflected by the density ratio of unburned gas to burned gas at two sides of the flame front ($\rho_u/\rho_b$) and flame thickness ($\delta_l$). Flame stability decreases with the increase of density ratios but increases with the increase of flame thickness. The combination of these two factors determines flame stability.

The relationships among density ratio (as well as flame thickness), hydrogen fraction, equivalence ratio and initial pressure are illustrated in Fig. 9. Flame thickness slightly decreases with the increase of hydrogen fraction and initial pressure for the mixtures from lean to rich; while density ratio obviously declines with the increase of hydrogen fraction and is hardly affected by the change of initial

pressures within the range of our experiments. From Fig. 9, it can be seen that flame thickness decreases with the increase of initial pressure, which suggests that flame stability decreases under this situation. This trend agrees with the illustration of Figs. 7 and 8, which clearly shows that large amount of flaw and honeycomb-like surface appear with the increase of initial pressure at various equivalence ratios and hydrogen fractions.

## 5. Conclusions

In this paper, flame propagation characteristics of NG–hydrogen–air mixtures were studied in a constant volume combustion bomb at different initial pressures and equivalence ratios. The main conclusions are summarized as below:

1. Initial pressure, hydrogen fraction as well as equivalence ratio exert a combined influence on unstretched laminar burning velocity and mass burning flux of NG–hydrogen–air mixtures. Both unstretched laminar burning velocity and mass burning flux quickly increase with the increase of hydrogen fraction.
2. Flame stability decreases with the increase of hydrogen fraction and initial pressure. For the case of relatively low hydrogen fraction (20%), flame stability of relatively lean combustion decreases with the increase of initial pressure, while for the case of high hydrogen fraction (80%), flame stability of lean and stoichiometric combustion decreases with the increase of initial pressure.
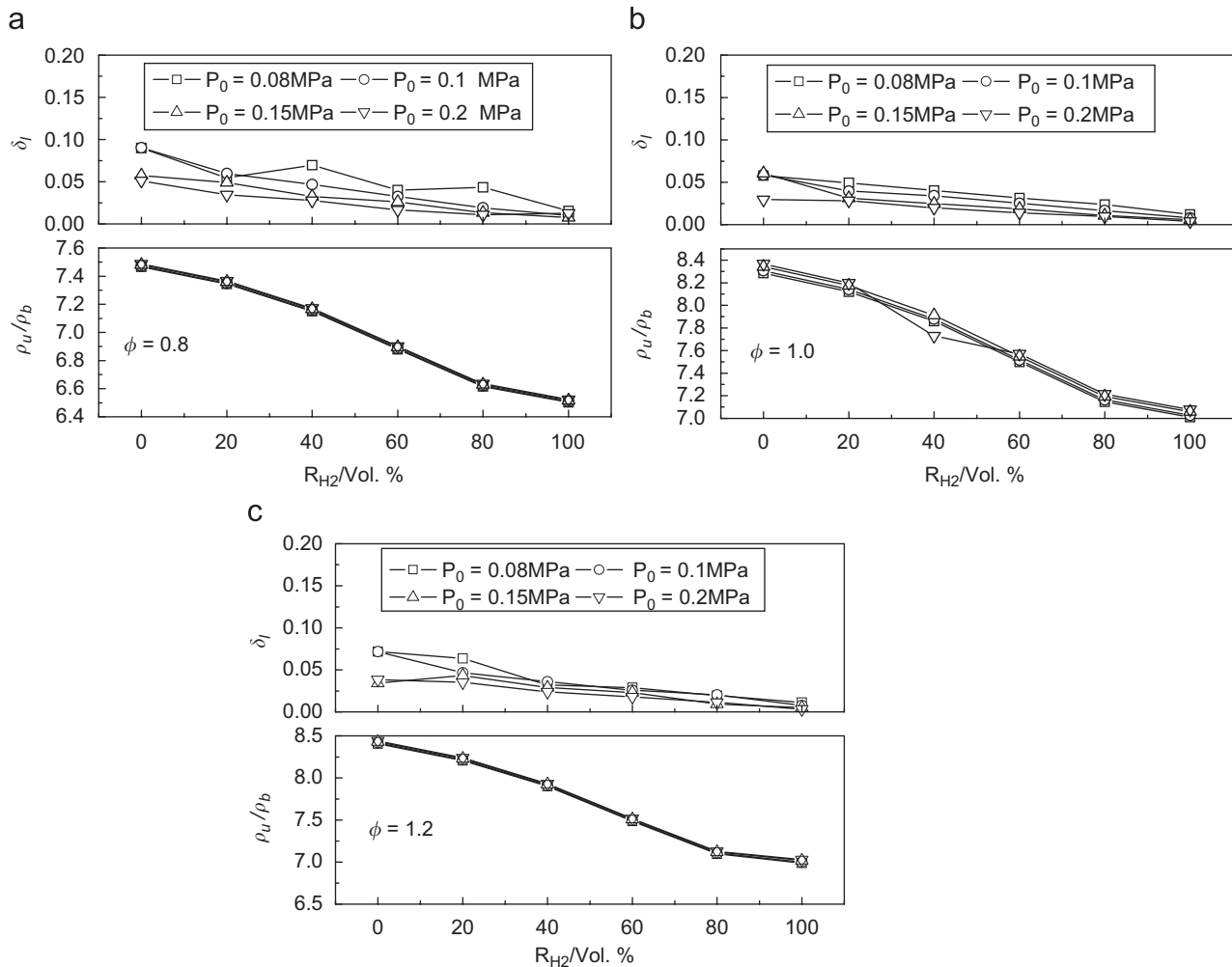
**Fig. 9 – Effects of initial pressure, hydrogen fraction and equivalence ratio on flame thickness and density ratio.**

3. At large flame radius, flame stability is dominantly influenced by hydrodynamic factors, reflected by both density ratios of unburned gas to burned gas at two sides of flame front and flame thickness. For fixed equivalence ratio and hydrogen fraction, the increase of initial pressure has obvious influence on flame thickness but slight influence on density ratio, that is, flame thickness decreases with the increase of initial pressure, indicating that flame stability decreases with the increase of initial pressure.

## Acknowledgments

REFERENCES

[1] Gold T. Earth outgassing of methane, methane fuel for the future. In: McGeer P, Durbin E, editors. New York: Plenum Press; 1982.

[2] Akansu S, Dulger A, Kahraman N, et al. Internal combustion engines fueled by natural gas–hydrogen mixtures. Int J Hydrogen Energy 2004;29(14):1527–39.

[3] Gu X, Haq M, Lawes M, et al. Laminar burning velocity and Markstein lengths of methane–air mixtures. Combust Flame 2000;121(1–2):41–58.

[4] Lamoureux N, Djebaili-Chaumeix N, Paillard C. Laminar flame velocity determination for $H_2$–air–He–$CO_2$ mixtures using the spherical bomb method. Exp Therm Fluid Sci 2003;27(4):385–93.

[5] Liao S, Jiang D, Cheng Q. Determination of laminar burning velocities for natural gas. Fuel 2004;83(9): 1247–50.

[6] Yu G, Law C, Wu C. Laminar flame speeds of hydrocarbon+air mixtures with hydrogen addition. Combust Flame 1986;63(1–2):339–47.

[7] Halter F, Chauveau C, Djebayli-Chaumeix N. Characterization of effects of pressure and hydrogen concentration on laminar burning velocities of methane–hydrogen–air mixture. Proc Combust Inst 2005;30:201–8.

[8] Law C, Kwon O. Effects of hydrocarbon substitution on atmospheric hydrogen–air flame propagation. Int J Hydrogen Energy 2004;29(8):867–79.

[9] Huang Z, Zhang Y, Zeng K, Liu B, Wang Q, Jiang D. Measurements of laminar burning velocities for natural gas–hydrogen–air mixtures. Combust Flame 2006;146: 302–11.

[10] Kwon O, Rozenchan G, Law C. Cellular instability and self-acceleration of outwardly propagation spherical flames. P Combust I 2002;29:1775–83.

[11] Bradley D, Gaskell P, Gu X. Burning velocities, Markstein lengths, and flame quenching for spherical methane–air flames: a computational study. Combust Flame 1996;104(1–2):176–98.

[12] Bradley D, Hicks R, Lawes M, Sheppard C, Woolley R. The measurement of laminar burning velocities and Markstein numbers for iso-octane–air and iso-octane–n-heptane–air mixtures at elevated temperatures and pressures in an explosion bomb. Combust Flame 1998;115:126–44.

[13] Jiang D, Chen C, Yang J, Yang Z. Advanced internal combustion engines fundamentals. Xi'an Jiaotong University Press; 2007.

[14] Westbrook C, Dryer F. Prediction of laminar flame properties of methanol–air mixtures. Combust Flame 1980; 37:171–92.